

The Adiabatic Correction Factor for Deformation Heating During the Uniaxial Compression Test

R.L. Goetz and S.L. Semiatin

(Submitted 11 June 2001)

The isothermal uniaxial compression test is a common method to determine the flow stress of metals. For accurate flow stress data at strain rates $>10^{-3} \text{ s}^{-1}$, the data must be corrected for flow softening due to deformation heating. The first step in the correction is to determine the increase in temperature. An adiabatic correction factor, η , is used to determine the temperature between strain rates of 10^{-3} to 10^1 s^{-1} . The adiabatic correction factor is the fraction of adiabatic heat retained in the workpiece after heat loss to the dies, $\eta = (\Delta T_{\text{ACTUAL}})/(\Delta T_{\text{ADIABATIC}})$, where $\Delta T_{\text{ADIABATIC}} = (0.95 \int \sigma d\epsilon)/(\rho C_p)$. The term η is typically taken to be constant with strain and to vary linearly (0 to 1) with $\log(\dot{\epsilon})$ between 10^{-3} and 10^1 s^{-1} . However, using the finite element method (FEM) and a one-dimensional, lumped parameter method, η has been found to vary with strain, die and workpiece thermal conductivities, and the interface heat-transfer coefficient (HTC). Using the lumped parameter method, an analytical expression for η was derived. In this expression, η is a function of the die and workpiece thermal conductivities, the interface heat-transfer coefficient, workpiece heat capacity, strain, and strain rate. The results show that an increase in the HTC or thermal conductivity decreases η .

Keywords adiabatic correction, compression test, deformation heating, FEM process modeling, flow stress

1. Introduction

The uniaxial compression of a cylindrical specimen between flat dies is one of the most common methods of determining the flow stress and workability of an alloy. Due to strain rate and temperature sensitivity in the warm and hot working regime, a series of compression tests at various temperatures and strain rates are typically conducted to provide flow stress as a function of strain, strain rate, and temperature. These data can be correlated with microstructure evolution during the test to provide insight into the best possible processing route for the alloy given the constraints of tooling, desired product shape, and desired microstructure. Also, with the advent of powerful computer simulation tools, such as the finite element method (FEM), accurate flow stress data are a necessary input for the proper use of such software.

Flow softening is a common characteristic of stress-strain curves for various alloys, whereby the curve decreases after reaching a peak stress. This softening can be caused by microstructural changes in the alloy and deformation heating, either alone or together. Examples of microstructural changes are dynamic recrystallization in single-phase alloys, development or modification of texture, and globularization and lamellar reorientation in titanium aluminides (TiAl). Deformation heating, however, will occur in any alloy and is primarily a function

of the imposed strain rate. Deformation heating results in an increase in specimen temperature during the test, and the resulting flow stress will be lower than the actual flow stress for the desired test temperature under isothermal conditions.

Thus, the flow stress from compression tests must be corrected for deformation heating, although only for strain rates greater than 10^{-3} s^{-1} . At strain rates of 10^{-3} s^{-1} and lower, the amount of heat generated is usually very small and will be conducted away during the long time periods of the test so that the test is isothermal. The change in temperature is calculated using the following equation:

$$\Delta T = (\eta 0.95 \int \sigma d\epsilon)/(\rho C_p) \quad (\text{Eq 1})$$

where ΔT is the change in temperature, η is the adiabatic correction factor, $\int \sigma d\epsilon$ is the area under the uncorrected stress-strain curve, ρ is the density, C_p is the specific heat, and, together, ρC_p is known as the heat capacity or the volume specific heat. The factor of 0.95 is the fraction of mechanical work transformed to heat, with the remaining fraction going to microstructural changes. This factor is typically taken to be 0.9 to 0.95.

The adiabatic correction factor, η , is used between the isothermal conditions at strain rates $\leq 10^{-3} \text{ s}^{-1}$, where $\eta = 0$, and the adiabatic conditions at rates $\geq 10^1 \text{ s}^{-1}$, where $\eta = 1$. The adiabatic correction factor is the fraction of adiabatic heat retained in the workpiece due to heat loss to the dies and is defined as

$$\eta = (\Delta T_{\text{ACTUAL}})/(\Delta T_{\text{ADIABATIC}}) \quad (\text{Eq 2})$$

At strain rates between 10^{-3} and 10^1 s^{-1} , η has typically been taken to vary linearly with $\log(\dot{\epsilon})$,^[1,2] i.e., η is equal to 0.0, 0.25, 0.50, 0.75, and 1.0 for rates of 10^{-3} , 10^{-2} , 10^{-1} , 10^0 , and 10^1 s^{-1} , respectively. In general, η has been considered to be

R.L. Goetz Materials and Processes Division, UES Inc., 4401 Dayton-Xenia Road, Dayton, OH 45432-1894 and S.L. Semiatin Air Force Research Laboratory, Materials and Manufacturing Directorate, AFRL/MLLM, Wright-Patterson Air Force Base, OH 45433-7817. Contact e-mail: robert.goetz@wpafb.af.mil.

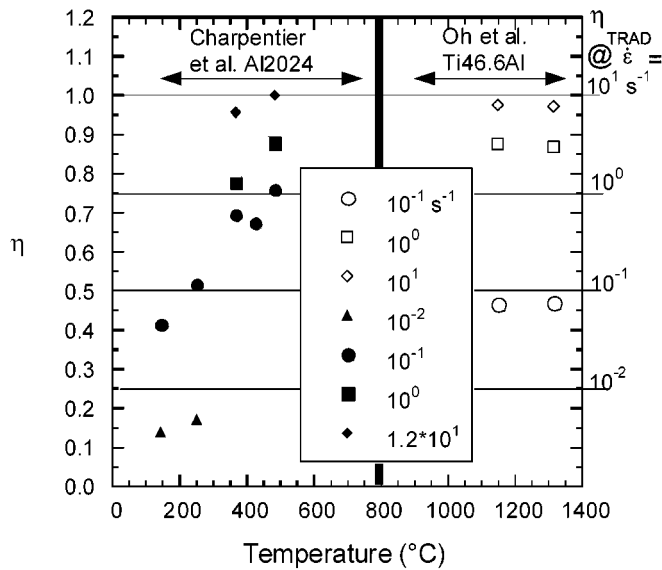


Fig. 1 Adiabatic correction factors, η , vs temperature at a strain of 0.7 from the research of Charpentier *et al.*^[3] and Oh *et al.*^[4] with traditional correction factors, η_{TRAD} of 0.25, 0.50, 0.75, and 1.0 at 10^{-2} , 10^{-1} , 10^0 , and 10^1 s^{-1}

independent of strain and temperature. However, compression tests on Al2024 by Charpentier *et al.*^[3] found that at a strain of 0.7, η differed from the typical values of η shown above, and in one case, η varied greatly with temperature (Fig. 1). For example, at 10^{-1} s^{-1} , η ranged from 0.4 to 0.75 rather than the typical value of 0.50. And at 10^{-2} s^{-1} , η was 0.14 and 0.17 instead of the expected 0.25. Oh *et al.*^[4] also calculated η at a strain of 0.7 for a TiAl alloy and found good agreement at rates of 10^{-1} s^{-1} ($\eta = 0.46$) and 10^1 s^{-1} ($\eta = 0.97$), and poor agreement at 10^0 s^{-1} ($\eta = 0.87$, Fig. 1). Oh *et al.* also showed that η was relatively insensitive to the interface friction factor. It has also been assumed that η does not vary with strain. However, during the correction of flow stress for a fully lamellar TiAl alloy undergoing severe microstructural flow softening and compressed to very large strains of 1.4, Goetz and Seetharaman^[5] found that η does vary with strain.

In light of the above research, which has found that η can vary with temperature and strain in addition to strain rate, the present work will investigate the factors that determine η using a finite element program and a one-dimensional (1-D) analytical approach. The effect of thermal properties of the workpiece and dies on η will be examined, as well as the interface between the die and workpiece and the workpiece flow stress.

2. Procedure

The finite element program DEFORM[™] (Scientific Forming Technologies Corporation, Columbus, OH) was used to model the uniaxial compression test under two-dimensional/axisymmetric/nonisothermal conditions. Because η is only applicable to the correction of flow stress for deformation heating between isothermal (10^{-3} s^{-1}) and adiabatic conditions (10^1 s^{-1}), constant strain rates of 10^{-2} , 10^{-1} , 10^0 , and 10^1 s^{-1} were used. An exponential decay for the instantaneous die velocity was used:

Table 1 Material thermal properties

| Material | ρC_p , N/mm ² °C | K, N/s °C |
|---|-----------------------------------|-----------|
| SiC ^[4] | 3.88 | 20.97 |
| Si ₃ N ₄ ^[9] (RBSN) ^(a) (1000 °C) | 3.44 | 2.0 |
| Si ₃ N ₄ ^[9] (HPSN) ^(b) (1000 °C) | 3.44 | 10.0 |
| OFHC Cu ^[10] | 3.44 | 391.0 |
| TiAl at 800 °C | 3.06 | 25.50 |
| 900 °C | 3.06 | 24.41 |
| 1000 °C | 3.10 | 23.32 |
| 1100 °C | 3.50 | 22.23 |
| 1200 °C | 4.40 | 21.14 |

(a) RBSN—Reaction Bonded Silicon Nitride
(b) HPSN—Hot Pressed Silicon Nitride

Table 2 Simulation conditions

| | |
|---------------------------------------|---|
| Initial temperature | 1093 °C |
| Constant shear stress friction factor | 0.0 |
| Emissivity (specimen) | 0.65 |
| Emissivity (dies) | 0.80 |
| Interface HTC | 10 kW/m ² °C ^[13] 25 kW/m ² °C ^[4] |
| Convection HTC | 0.02 kW/m ² °C |

$$V_i = \dot{\epsilon} H_0 \exp(-\dot{\epsilon} t) \quad (\text{Eq 3})$$

where V_i is the instantaneous die velocity, $\dot{\epsilon}$ is the strain rate, H_0 is the initial specimen height, and t is time. For each strain rate, two simulations were conducted: (1) completely nonisothermal with heat transfer from the compression specimen to the dies and the environment to simulate actual test conditions; and (2) completely adiabatic with nonisothermal conditions in the specimen, but no heat transfer to the dies or the environment. The average specimen temperature was then determined for each strain to calculate η using Eq 2. Stress-strain curves were calculated using the FEM load-stroke curves and the die/specimen contact area, assuming a uniform specimen without barreling.

The material used for the compression specimen was a TiAl alloy with the following flow stress (σ) constitutive equation:

$$\sigma = A \dot{\epsilon}^m \exp(Qm/RT) \quad (\text{Eq 4})$$

where $A = 0.5874$ MPa; the strain rate sensitivity, $m = 0.2$; the activation energy, $Q = 400$ kJ/g mole; the universal gas constant, $R = 8.3144$ J/g mole K; and the temperature is T (K). As shown, the flow stress is both strain rate and temperature sensitive, but constant with strain. A strain sensitive material with flow softening due to microstructural softening effects was not used, so that deformation heating would be the sole cause of flow softening.

A uniform initial temperature of 1093 °C was used for the specimen, dies, and ambient temperature. The cylindrical specimen dimensions were 10.16-mm diameter \times 15.24-mm height for the standard height-to-diameter ratio of 1.5. The specimen FEM mesh consisted of 1064 nodes and 990 elements. Silicon

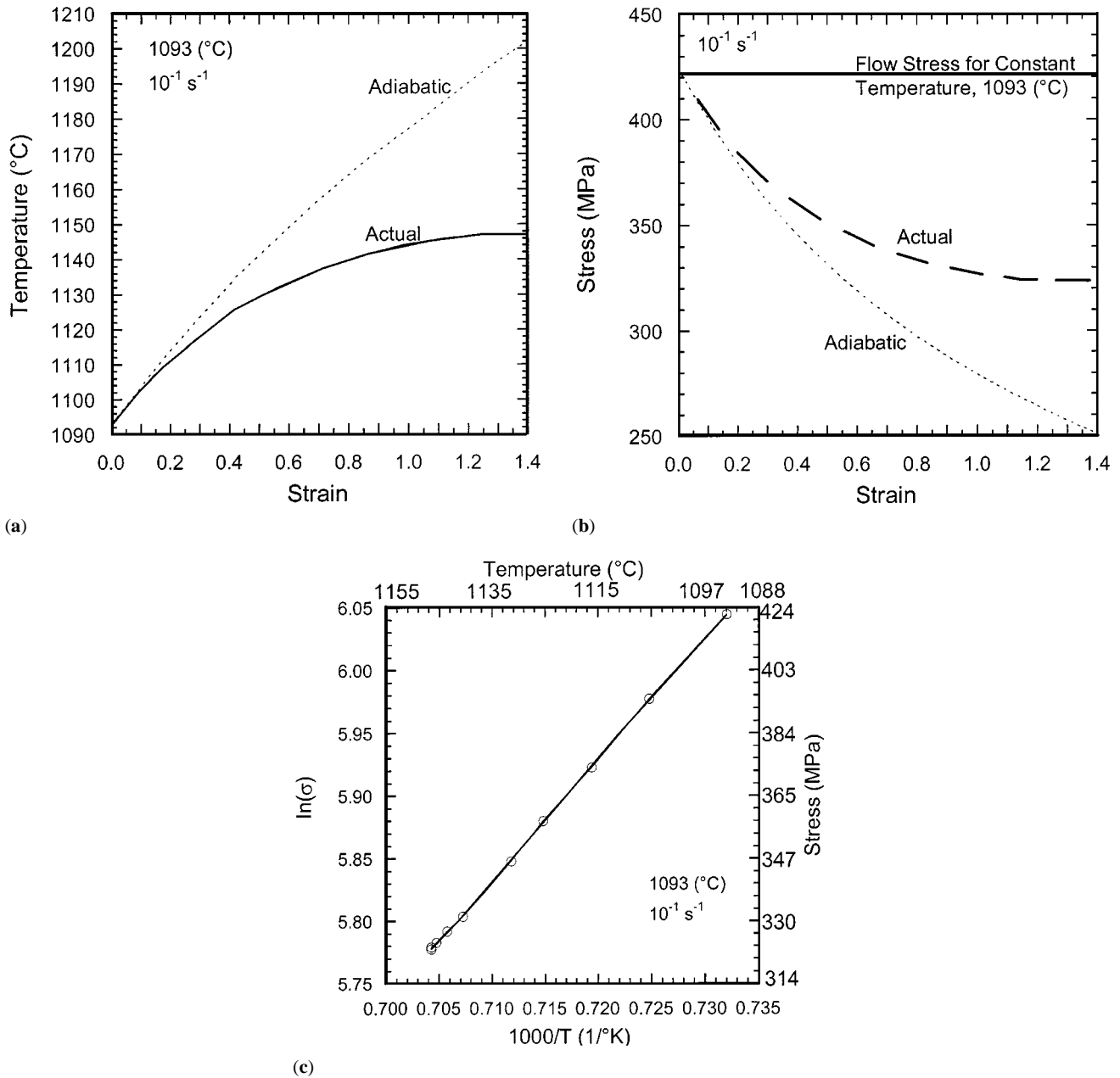


Fig. 2 (a) FEM temperature changes and (b) flow stress softening as functions of strain for adiabatic and actual conditions at 10^{-1} s^{-1} with RBSN dies ($K = 2.0 \text{ N/s } ^\circ\text{C}$). (c) The $\ln(\sigma)$ vs $1000/(1093 + (\Delta T + 273), \text{ K})$ plot, which is an example of the method to determine the corrected flow stress using ΔT

nitride (Si_3N_4) and silicon carbide (SiC) dies 100.0-mm diameter \times 25.0-mm height were used with an FEM mesh of 780 nodes and 722 elements. The applicable thermal properties of heat capacity and thermal conductivity, as well as simulation conditions, can be found in Tables 1 and 2.

3. Results and Discussion

3.1 The FEM

Temperatures and stresses for the 10^{-1} s^{-1} compression test simulation are shown in Fig. 2(a) and (b) plotted versus strain.

As expected, the temperatures are lower for actual compression test conditions than for adiabatic conditions, due to heat loss to the dies and the environment. Because of the lower temperatures in actual test conditions, the resulting stresses are higher than those of the adiabatic test conditions (Fig. 2b). Figure 2(b) also shows the flow stress for the (hypothetical) isothermal test. The difference between this curve and the stress-strain curve from the actual compression test simulation shows the amount of correction needed due to deformation heating. This would be accomplished by plotting $\ln(\sigma)$ vs $1000/T \text{ K}^{-1}$ (Fig. 2c), where T is the absolute, instantaneous temperature during the test, and extrapolating back to the initial test temperature to find

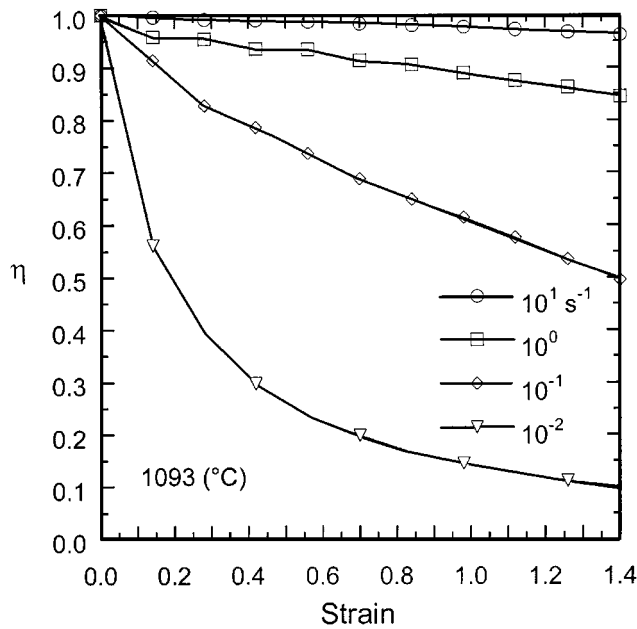


Fig. 3 A plot of η vs strain for strain rates of 10^{-2} , 10^{-1} , 10^0 , and 10^1 s^{-1} with RBSN dies ($K = 2.0$ N/s $^{\circ}C$) and an HTC of 10 kW/m^2 $^{\circ}C$ using FEM

the corrected flow stress. Since there is no strain dependence of the flow stress in the constitutive equation used here (Eq 4), flow stress correction would only require data from one test temperature. For strain-dependent alloys, which also undergo microstructural flow softening, a $\ln(\sigma)$ versus $1000/T$ correction plot for each selected strain from the stress-strain curve would be made using the uncorrected stresses and instantaneous temperatures from each nominal test temperature in the test matrix.^[2]

Previous work involving the flow stress correction for a fully lamellar TiAl alloy^[5] found that η varied with strain as well as strain rate. Using the constitutive equation of Section 2 (Eq 4), thermal properties for reaction bonded silicon nitride (RBSN) dies, and an interface heat-transfer coefficient (HTC) of 10 kW/m^2 $^{\circ}C$, η was calculated and plotted versus strain for several strain rates (Fig. 3). As in the previous work,^[5] Fig. 3 also demonstrates that η varies with strain. The values for η at a strain of 0.7 can be compared to the work of Charpentier *et al.*^[3] and Oh *et al.*^[4] shown in Fig. 1. The results in Fig. 3 for strain rates of 10^{-2} s^{-1} , 10^0 s^{-1} , and 10^1 s^{-1} compare well with Charpentier. The results at 10^{-1} s^{-1} also compare well with Charpentier for two of the five test temperatures (365 and 425 $^{\circ}C$). At 10^{-1} s^{-1} , however, Charpentier found that temperature greatly affected η (0.414 to 0.759), and these η 's do not compare well with Fig. 3. As with Charpentier, the results in Fig. 3 also compare well with Oh at 10^0 and 10^1 s^{-1} . However, the results for 10^{-1} s^{-1} ($\eta = 0.69$) do not agree with Oh ($\eta \approx 0.47$).

The possible causes for the differences with Oh *et al.*^[4] at 10^{-1} s^{-1} can be found by comparing material properties and interface heat-transfer coefficients. As a first check, the η 's from Oh *et al.* were duplicated by using the same material properties, constitutive equation, and simulation conditions as Oh *et al.* Once the η 's from Oh *et al.* were duplicated, the

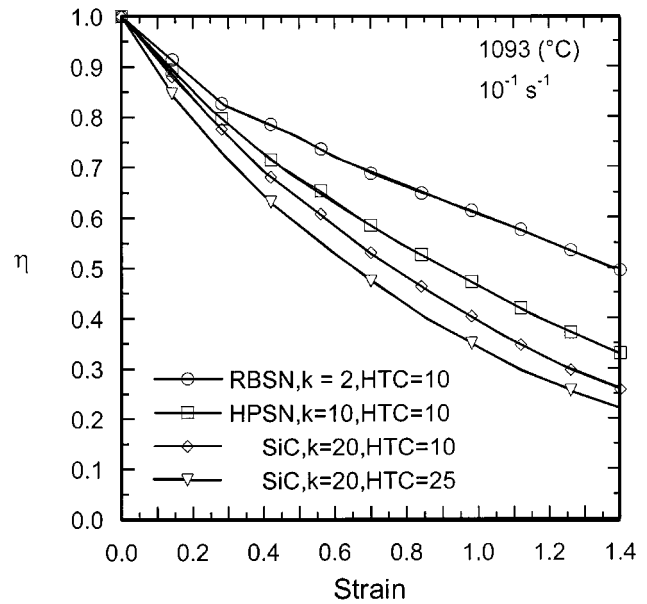


Fig. 4 A plot of η vs strain at 10^{-1} s^{-1} showing the effect of die thermal conductivity, K , and interface HTC on η for RB Si_3N_4 , HP Si_3N_4 , and SiC dies with HTC = 10 and 25 kW/m^2 $^{\circ}C$ using FEM

differences between simulation conditions used by Oh *et al.* and the present work were examined. The present work and that of Oh used TiAl compression specimens of the same size and approximately equal heat capacities and thermal conductivities; therefore, the difference lies in the constitutive equations, die materials, and/or interface (HTCs). Oh *et al.* used SiC dies with a thermal conductivity (K) of 20.97 N/s $^{\circ}C$ and an HTC of 25 kW/m^2 $^{\circ}C$, while the present work initially used die material properties for reaction bonded silicon nitride (RBSN, $K = 2.0$ N/s $^{\circ}C$, Table 1) and an HTC of 10 kW/m^2 $^{\circ}C$. More applicable silicon nitride properties would have been for hot-pressed silicon nitride, which was used in the earlier work^[5] (HPSN, $K = 10$ N/s $^{\circ}C$), rather than for RBSN.

In addition to the die thermal conductivities and HTCs, it was found that Oh *et al.*^[4] used an activation energy (Q) of 626.8 kJ/g mole in their TiAl constitutive equation. This was much larger than the Q used in the present work ($Q = 400$ kJ/g mole). In both constitutive equations, Q affects the temperature sensitivity of the alloy. To determine if Q , and in turn the flow stress temperature sensitivity, affected η , the activation energy in the present constitutive equation was reduced to 300 kJ/g mole. Changing the temperature sensitivity in this manner did not affect η . Thus, the value of Q is not believed to be the difference between Oh *et al.* and the present work. This leaves the die material properties and the HTC as possible differences.

The effect of the various die material properties and HTCs on η using the TiAl of Eq 4 at 10^{-1} s^{-1} can be seen in Fig. 4. The effect is that the larger K of SiC and the larger HTC of 25 kW/m^2 $^{\circ}C$ lowers the thermal resistance, allowing greater heat flow from the specimen, which decreases the specimen temperature, and thereby lowers η . Using SiC dies and an HTC of 25 kW/m^2 $^{\circ}C$ results in an η equal to that of Oh *et al.* Figure 5 shows η versus strain for rates of 10^{-2} , 10^{-1} , 10^0 , and 10^1 s^{-1}

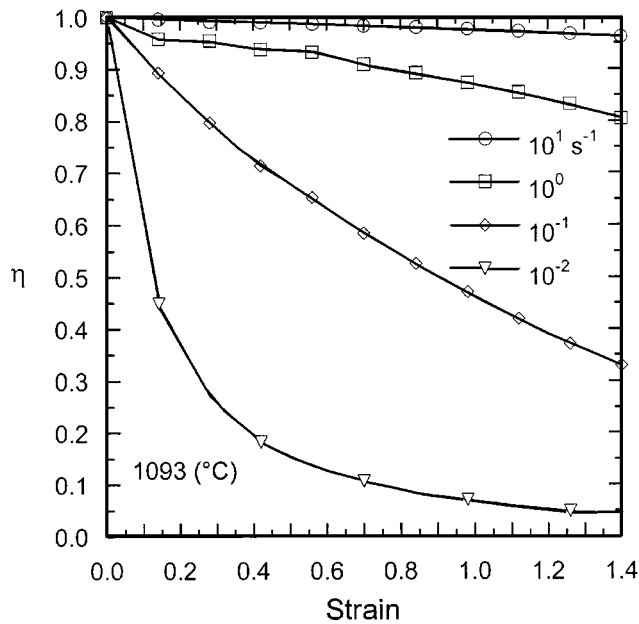


Fig. 5 A plot of η vs strain for strain rates of 10^{-2} , 10^{-1} , 10^0 , and 10^1 s^{-1} with appropriate HPSN dies ($K = 10.0$ N/s $^{\circ}C$) and an HTC of 10 kW/m^2 $^{\circ}C$ using FEM

for the more appropriate HPSN dies used in previous experimental compression tests^[5] and an HTC of 10 kW/m^2 $^{\circ}C$.

The above results confirm the work of Goetz and Seetharaman^[5] that in addition to changing with strain rate, η does decrease with strain from an initial value of 1.0. How do the traditionally used constant values of η [0.0 (10^{-3} s^{-1}), 0.25 (10^{-2} s^{-1}), 0.50 (10^{-1} s^{-1}), 0.75 (10^0 s^{-1}), and 1.0 (10^1 s^{-1})] affect the temperature values used in the correction of the flow stress? A comparison of the actual temperatures and the temperatures calculated using the constant η 's multiplied by the adiabatic temperatures can be seen in Fig. 6. For rates of 10^{-2} and 10^{-1} s^{-1} (Fig. 6a and b), a constant η would underestimate the temperature for small strains and then overestimate it for larger strains. The transition from under to overestimation occurs at a strain of approximately 0.7, where the error would be minimal. However, at strains greater than 0.7, the error would be large. For 10^0 s^{-1} (Fig. 6c), the error is large for most strains where a constant η of 0.75 underestimates the temperature.

The above results show the roles that die thermal properties and interface HTCs play in the temperature changes in a compression specimen during deformation. However, the results do not explain the change in η (0.414 to 0.759) with temperature shown by Charpentier *et al.*^[3] for Al2024 at 10^{-1} s^{-1} . The above results do show that η can vary from 0.47 to 0.69 due to changes in die thermal conductivities and HTCs. Charpentier *et al.* used a superalloy for dies in all tests, and most superalloys have a thermal conductivity very close to that of SiC (Table 3). Also, the thermal properties would not change greatly in this temperature range, so this could not be the source of changes in η .

Another difference with the work of Charpentier *et al.*^[3] is the Al2024 compression specimens. Aluminum alloys have very high thermal conductivities ($K_{2024-0} \approx 190$ N/s $^{\circ}C$),^[10]

Table 3 Die material thermal conductivities

| Material | K , N/s $^{\circ}C$ (temperature, $^{\circ}C$) |
|--|---|
| H13 ^[11] | 24.6 (215), 24.7 (605) |
| IN100 ^[11] | 17.3 (538) |
| IN713 ^[11] | 10.9(93), 17(538), 26.4(1093) |
| IN718 ^[11] | 11.4(93), 19.6(538), 24.9(871) |
| SiC ^[4] | 20.97 (1149) |
| Si ₃ N ₄ ^[9] (HPSN) | 10.0 (1000) |
| Molybdenum ^[12] | 130 (426), 105 (871), 90 (1760), 75 (1760), 70 (2204) |

especially when compared to the TiAl alloy used here and titanium alloys in general, which have the lowest thermal conductivities of all engineering alloys. Figure 7 compares η versus strain curves for TiAl and OFHC Cu at 10^{-1} s^{-1} . Other than silver, OFHC Cu has the highest thermal conductivity of any engineering metal ($K = 391$ N/s $^{\circ}C$). At a strain of 0.7, the OFHC Cu curve has an η of 0.39, which compares with the lowest value of η at 10^{-1} s^{-1} by Charpentier *et al.*

The results discussed in this section show the degree to which η is affected by workpiece and die material properties and interface HTCs. Since η is used to correct compression test flow stress data, the accuracy of these data would be affected.

3.2 An Analytical Expression for the Adiabatic Correction Factor— η

An analytical expression for η would be useful in light of the above results, which have shown that in addition to strain rate, η depends on strain, thermal properties, and HTCs. A 1-D lumped parameter model,^[6,7] shown schematically in Fig. 8, was used to develop an expression for η . The derivation of the equations follows and is based on one-half of the workpiece volume.

$$q_{DIS} = hA(T_{HT} - 1093 \text{ } ^{\circ}C) \quad (\text{Eq } 5)$$

$$h = [x_W/K_W + 1/HTC + x_D/K_D]^{-1} \quad (\text{Eq } 6)$$

The power dissipated from the workpiece to the dies, q_{DIS} , is given by Eq 5, where A is the interface contact area, T_{HT} is the workpiece temperature, and 1093 $^{\circ}C$ is the interior die temperature. The term "h" (Eq 6) is an overall HTC that "lumps" together the thermal resistances of the workpiece interior, workpiece/die interface contact area, and the die interior, where x_W is one-half the workpiece height, K_W is the workpiece thermal conductivity, HTC is the interface heat-transfer coefficient, x_D is the distance from the die surface to the die interior where temperature is constant, and K_D is the die thermal conductivity. Equations 7 and 8

$$x_W = X_0 \exp(-\dot{\epsilon}t) \quad (\text{Eq } 7)$$

$$A = V/x_W \quad (\text{Eq } 8)$$

are one-half the workpiece height and interface contact area, where X_0 is the initial half-height, $\dot{\epsilon}$ is the strain rate, t is time, and V is one-half the total specimen volume. The change in

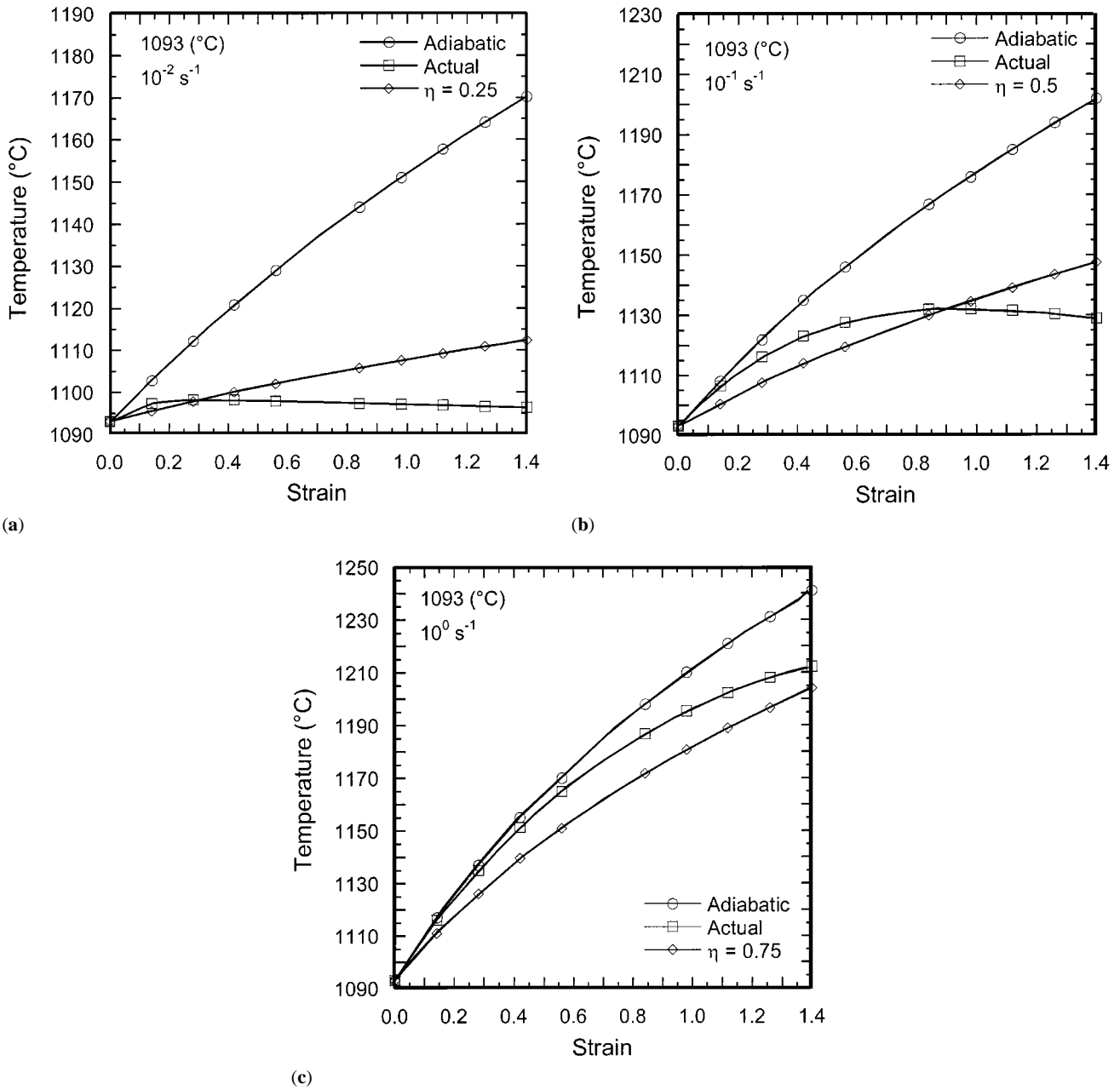


Fig. 6 A comparison between adiabatic FEM temperatures, actual FEM temperatures, and corrected FEM temperatures calculated using the traditional constant η 's and the errors from using them: (a) 10^{-2} s^{-1} ($\eta = 0.25$), (b) 10^{-1} s^{-1} ($\eta = 0.50$), and (c) 10^0 s^{-1} ($\eta = 0.75$)

the internal energy of the workpiece is given below on the left of Eq 9, where it is the difference between the internal power generated by deformation, q_{DEF} (Eq 10), and the power dissipated to the dies, q_{DIS} (Eq 5):

$$(V\rho C_p) \frac{dT_{\text{HT}}}{dt} = q_{\text{DEF}} - q_{\text{DIS}} \quad (\text{Eq 9})$$

$$q_{\text{DEF}} = (\sigma)(\dot{\epsilon})(V) \quad (\text{Eq 10})$$

$$dT_{\text{HT}} = T_{\text{HT}} - 1093 \text{ }^\circ\text{C} \quad (\text{Eq 11})$$

$$dT_{\text{HT}} = (\sigma)(\dot{\epsilon})dt / (\rho C_p) - hA(dT_{\text{HT}})(dt) / (V\rho C_p) \quad (\text{Eq 12})$$

$$dT_{\text{HT}} + hA(dT_{\text{HT}})(dt) / (V\rho C_p) = (\sigma)(\dot{\epsilon})(dt) / (\rho C_p) \quad (\text{Eq 13})$$

$$dT_{\text{HT}}[1 + hA(dt) / (V\rho C_p)] = (\sigma)(\dot{\epsilon})(dt) / (\rho C_p) \quad (\text{Eq 14})$$

By substituting Eq 10 and 11 into Eq 9, manipulation (Eq 12 to 14) results in the change in temperature of the workpiece:

$$dT_{\text{HT}} = [(\sigma)(\dot{\epsilon})(dt) / (\rho C_p)] \cdot [1 + hA(dt) / (V\rho C_p)]^{-1} \quad (\text{Eq 15})$$

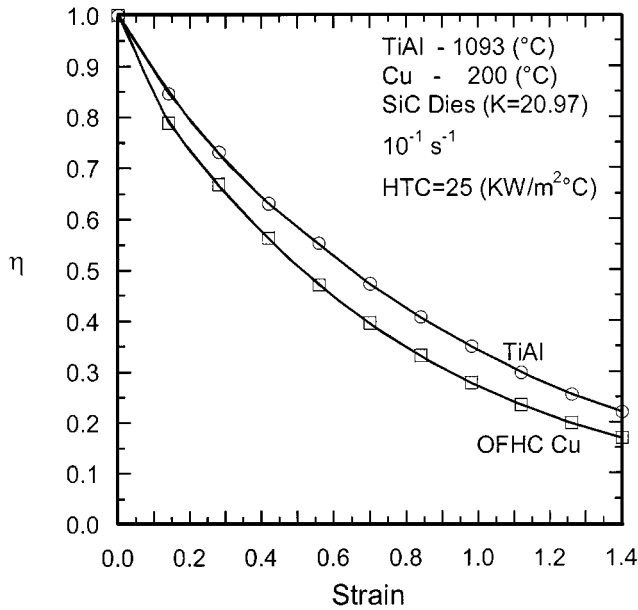


Fig. 7 Plots of η vs strain at 10^{-1} s^{-1} comparing the effect of alloy thermal conductivity on η with TiAl ($K = 22 \text{ N/s } ^\circ\text{C}$) and OFHC Cu ($K = 391 \text{ N/s } ^\circ\text{C}$), SiC ($K = 20.97 \text{ N/s } ^\circ\text{C}$) dies, and an $\text{HTC} = 25 \text{ kW/m}^2 \text{ } ^\circ\text{C}$ using FEM

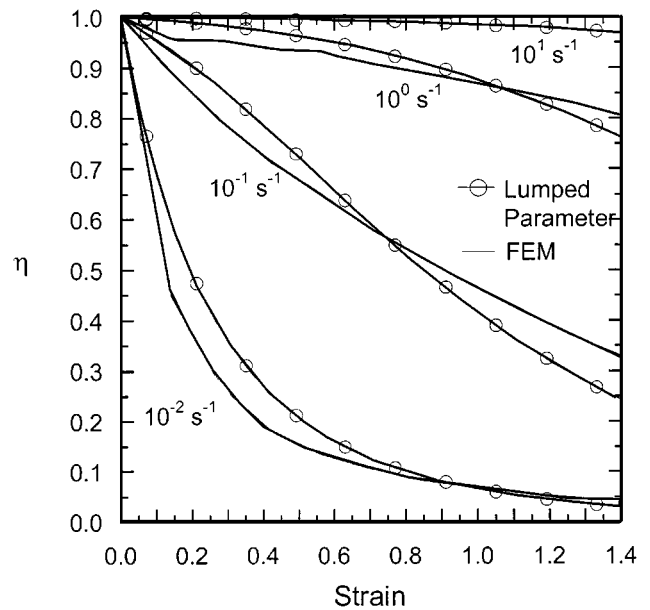


Fig. 9 A plot of η vs strain for strain rates of 10^{-2} , 10^{-1} , 10^0 , and 10^1 s^{-1} comparing FEM and lumped parameter results for TiAl ($K_W = 22 \text{ N/s } ^\circ\text{C}$), HPSN dies ($K_D = 10.0 \text{ N/s } ^\circ\text{C}$, $x_D = 5.0 \text{ mm}$), and an HTC of $10 \text{ kW/m}^2 \text{ } ^\circ\text{C}$

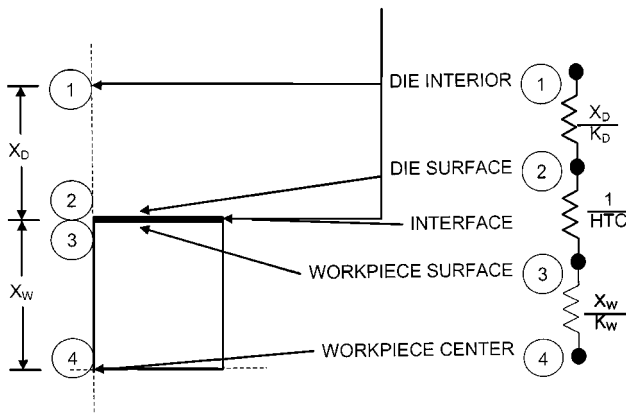


Fig. 8 Schematic diagram of a 1-D lumped parameter model

The change in temperature for adiabatic conditions alone, dT_{ADIAB} , is simply Eq 9 without power dissipation, q_{DIS} :

$$dT_{\text{ADIAB}} = (\sigma)(\dot{\epsilon})(dt)/(\rho C_p) \quad (\text{Eq 16})$$

with dT_{HT} and dT_{ADIAB} derived, Eq 15 and 16 can be inserted into Eq 2 to determine η

$$\eta = (\Delta T_{\text{HT}})/(\Delta T_{\text{ADIAB}}) = \int dT_{\text{HT}}/\int dT_{\text{ADIAB}} \quad (\text{Eq 17})$$

This results in the cancelation of the $[(\sigma)(\dot{\epsilon})(dt)/(\rho C_p)]$ term leaving

$$\eta = [1 + hA(\Delta t)/(V\rho C_p)]^{-1} \quad (\text{Eq 18})$$

and with $\Delta t = \Delta\epsilon/\dot{\epsilon}$ and $A = V/x_W$ (Eq 8), substitution leaves the final form of η :

$$\eta = [1 + (h\Delta\epsilon)/(x_W\rho C_p\dot{\epsilon})]^{-1} \quad (\text{Eq 19})$$

When Eq 19 for η is plotted versus strain for rates of 10^{-2} , 10^{-1} , 10^0 , and 10^1 s^{-1} , the agreement with the FEM calculated η 's is very good (Fig. 9). Equations 19 and 6 give approximate quantitative values for η and show the qualitative effects of K , HTC , ρC_p , strain, and strain rate on η . For example, increasing the HTC or the K s increases the overall HTC , h , which in turn decreases η . This agrees with the FEM results discussed in the previous section and shown in Fig. 4 and 7. The opposite occurs with an increase in the heat capacity, ρC_p , where η increases. The major effect on η , however, as shown by the effect of strain rate, is the ratio of $\Delta\epsilon/\dot{\epsilon}$, which is the elapsed time for heat transfer to occur.

Thermal properties such as ρC_p and K are generally a function of temperature, which makes η a function of temperature also. For most alloys, ρC_p increases with temperature, which would cause η to increase. However, K usually decreases with temperature, which would also cause an increase in η . It is also possible that the HTC decreases with temperature. Because an alloy's flow stress decreases with temperature, more lubricant would be retained at the interface and the HTC would be lower. A decreasing HTC with temperature would also cause η to increase with temperature. Thus, the effect of changing temperature on the thermal properties and the HTC could cause η to increase with temperature, something found experimentally by Charpentier *et al.*^[3]

Just as the thermal properties of ρC_p and K change with temperature, which in turn changes η , ρC_p and K also change with metals and alloys. Thus, the combination of workpiece

and die alloys can also affect η . However, Ashby^[8] has shown that ρC_p does not vary greatly. For engineering alloys, the average ρC_p is 3.0 N/mm² °C, ranging between 2.5 and 7.5 N/mm² °C. Also, with respect to affecting η , ρC_p only affects possible workpiece alloys, not die alloys. Thermal conductivities, however, apply to both workpiece and die alloys and can vary almost two orders of magnitude, from Ti alloys at the lower bound with $K \approx 8$ N/s °C to Cu at the upper bound with $K \approx 391$ N/s °C. However, K for typical die alloys ranges from 10 to 25 N/s °C, (Table 3). Only molybdenum, which is the main element in very high-temperature TZM alloy dies, lies outside this range with very high K s (70 to 130, N/s °C).

4. Conclusions

- For a given strain rate, the adiabatic correction factor (η) is not constant with strain, but decreases with increasing strain from an initial value of 1.0.
- The term η is a function of the die and workpiece thermal conductivities (K) and the interface HTC.
- The term η is not affected by the activation energy (Q) of the workpiece material. Since the flow stress temperature sensitivity ($d\sigma/dT$) is related to Q , $d\sigma/dT$ does not affect η .
- An analytical expression for η was derived based on a 1-D lumped parameter approach:

$$\eta = 1/[1 + (h\Delta\varepsilon)/(x_W\rho C_p\dot{\varepsilon})]$$

$$h = 1/[x_W/K_W + 1/HTC + x_D/K_D]$$

where x_W is one-half the workpiece height, ρ is the density, C_p is the specific heat, HTC is the interface heat-transfer coefficient, ε is the strain, $\dot{\varepsilon}$ is the strain rate, x_D is the distance from the die surface to the die interior, and K_W and K_D are workpiece and die thermal conductivities. This expression gives approximate quantitative values for η and shows the qualitative effects of K , HTC, ρC_p , strain, and strain rate on η .

- From the above equations for η and h , an increase in the

HTC or thermal conductivities results in a decrease in η . However, increasing ρC_p increases η .

- The effect of increasing temperature on the thermal properties and the HTC could cause η to increase with temperature.

Acknowledgments

This work was performed as part of the in-house research activities of the Processing Science Group, Materials and Manufacturing Directorate, Air Force Research Laboratory (Wright-Patterson AFB, OH). One of the authors (RLG) was supported by Air Force Contract No. F33615-96-C-5251. The authors also thank V.K. Seetharaman for helpful discussions during the course of this work.

References

1. P. Dadras and J.F. Thomas, Jr.: *Metall. Trans. A*, 1981, vol. 12A, pp. 1867-76.
2. J.F. Thomas, Jr. and R. Srinivasan: in *Computer Simulation in Materials Science*, R.J. Arsenault, J.R. Beeler, Jr., and D.M. Esterling, eds., ASM, Metals Park, OH, 1988, pp. 269-90.
3. P.L. Charpentier, B.C. Store, S.C. Ernest, and J.F. Thomas, Jr.: *Metall. Trans. A*, 1986, vol. 17A, pp. 2227-37.
4. S.I. Oh, S.L. Semiatin, and J.J. Jonas: *Metall. Trans. A*, 1992, vol. 23A, pp. 963-75.
5. R.L. Goetz and V. Seetharaman: Air Force Research Laboratory, Wright-Patterson AFB, OH, unpublished research, 1998.
6. E.O. Doebelin: *Systems Dynamics: Modeling and Response*, Charles E. Merrill, Columbus, OH, 1972, pp. 451-69.
7. J.P. Holman: *Heat Transfer*, 6th ed., McGraw-Hill, New York, NY, 1986, pp. 133-35.
8. M.F. Ashby: *Acta Metall.*, 1989, vol. 37, pp. 1273-93.
9. Anon.: *Engineered Materials Handbook: Ceramics and Glasses*, ASM International, Metals Park, OH, 1991, vol. 4, p. 815.
10. Anon.: *Metals Handbook: Properties and Selection: Nonferrous Alloys and Special-Purpose Materials*, 10th ed., ASM International, Metals Park, OH, 1990, vol. 2.
11. Anon.: *Metals Handbook: Properties and Selection: Irons, Steels, and High-Performance Alloys*, 10th ed., ASM International, Metals Park, OH, 1990, vol. 1.
12. Anon.: *Technical Data on Molybdenum*, The Rembar Company, Dobbs Ferry, NY, 1999, p. 3.
13. V.K. Jain and R.L. Goetz: *Determination of Contact Heat Transfer Coefficient for Forging of High Temperature Materials*, 91-HT-34, ASME, New York, NY, 1991.